Intramolecular Excimer Emissions of *syn*- and *anti*-[3.3](3,9)Carbazolophanes in Solutions†

Hideo Ohkita* and Shinzaburo Ito

Department of Polymer Chemistry, Graduate School of Engineering, Kyoto University, Yoshida, Sakyo, Kyoto 606-8501, Japan

Masahide Yamamoto

Faculty of Science and Engineering, Ritsumeikan University, Kusatsu, Shiga 525-8577, Japan

Yasuo Tohda and Keita Tani

Division of Natural Science, Osaka Kyoiku University, Asahigaoka, Kashiwara, Osaka 582-8582, Japan

Received: July 3, 2001; In Final Form: September 17, 2001

The photophysical properties of carbazole excimers were investigated using *syn*- and *anti*-[3.3](3,9)carbazolophanes: the *syn*-carbazolophane is a model compound for a fully overlapped carbazole excimer and the *anti*-carbazolophane for a partially overlapped carbazole excimer the structures of which have been determined by X-ray analysis. ^{1}H NMR spectra showed that two carbazole moieties in the *syn*- and *anti*-[3.3](3,9)carbazolophanes did not flip even in solution owing to short [3.3](3,9)linkage: geometrical alignments of two carbazole moieties remained the same as those determined by the X-ray analysis. Absorption bands of the carbazolophanes were broadened and blue- or red-shifted compared with those of 1,3-bis(3-methyl-*N*-carbazolyl)propane used as a reference compound. These spectral features were explained by Kasha's molecular exciton theory. Fluorescence spectra of both carbazolophanes were red-shifted, broad, and structureless bands. These broad emissions were ascribed to intramolecular excimer fluorescence of the carbazolophanes, which was insensitive to solvent polarity. The dipole moment in the excited state was estimated to be ∼0 D for the *anti*-carbazolophane and to be 4.8 D for the *syn*-carbazolophane from Lippert−Mataga plots. The radiative rate of excimer emission was 3.4×10^6 s^{-1} for the *anti*-carbazolophane and 7.2×10^5 s^{-1} for the *syn*-carbazolophane. Our [3.3](3,9)linkage carbazolophanes clearly showed that these different photophysical properties of carbazole excimers result from the geometries of their carbazole moieties.

1. Introduction

Since the first report[1] of the pyrene excimer in solution by Förster and Kasper in 1954, excimers have been studied by many researchers in the fields of photophysics and photochemistry.[2,3] The most prominent feature of excimer emission is the broad fluorescence band without a vibrational structure, the peak wavenumber of which is shifted about 6000 cm^{-1} lower than that of the monomer fluorescence. Birks and co-workers[4] pointed out that the energy difference is nearly constant (6000 cm^{-1}) for a large number of aromatic molecules. This energetic feature was interpreted in terms of a simple Hückel-type dimer orbital by Azumi et al.[5] Formation of intermolecular excimers in solution is diffusion-controlled: the formation depends on the viscosity of the solvent and the concentration of solute molecules. On the other hand, intramolecular excimers are independent of the concentration. Yanari and co-workers[6] were the first to report intramolecular excimers in a study of the fluorescence spectra of polystyrene in 1963. Almost at the same time, Hirayama[7] studied the fluorescence spectra of a variety of diphenyl and triphenyl alkanes in solution and found that intramolecular excimers can be formed only in those compounds in which two phenyl groups along a main alkane chain are separated by three carbon atoms ($n = 3$ rule). Rice and co-workers[8] studied the fluorescence and phosphorescence spectra of vinyl polymers using a number of model compounds of the diphenylalkane and paracyclophane series. Nishijima[9] proposed that excimer fluorescence provides a unique method for studying molecular configuration and conformation of polymer molecules. Ito and co-workers studied the intramolecular naphthalene excimers in detail from the viewpoint of kinetics, conformation, and thermodynamics.[10−13] Intramolecular excimers formed in polymer systems have been reviewed by Phillips[14] and Frank.[15]

Cyclophane chemistry has been opened by Cram.[16] He was the first to report a designed synthesis of [*m.n*]paracyclophanes.[17] The unique structure of cyclophanes has drawn the attention of many researchers in organic and physical chemistry. In the fields of photophysics and photochemistry, cyclophane is one of the most attractive molecules for studying the electronic interactions of face-to-face arranged aromatic rings. Absorption spectra of [*m.n*]paracyclophanes were systematically studied by Cram.[18] Emission spectra of [*m.n*]paracyclophanes have been experimentally and theoretically studied by many researchers.[8,19−22] Because paracyclophanes have a structure for which the geometrical arrangement of two aromatic rings is clearly defined, various cyclophanes (e.g., naphthalenophane,[23,24] anthracenophane,[25] pyrenophane,[26] phenanthrenophane[27,28]) have been studied to examine excimer properties on the basis of their structures.

† Part of the special issue "Noboru Mataga Festschrift".

* To whom correspondence should be addressed. E-mail: ohkita@polym.kyoto-u.ac.jp. Fax: +81-75-753-5632.

10.1021/jp0125146 CCC: $22.00
Published on Web 12/06/2001

Carbazole-related systems have been extensively studied compared with other aromatic compounds, because poly(*N*-vinylcarbazole) (PVCz) is one of the most sensitive photoconductive organic polymers.[29,30] Klöpffer investigated first the intramolecular excimer of 1,3-bis(*N*-carbazolyl)propane[31] as a model compound for PVCz, which shows excimer fluorescence both in dilute solution and in the solid state.[32] Johnson demonstrated that there exists a second excimer of which the emission band appears at a higher energy than that of the normal sandwich excimer.[33] Itaya and co-workers attributed the second excimer to a partially overlapped structure with only one eclipsed aromatic ring from two carbazolyl chromophores in the *tt* conformation of the syndiotactic sequence in PVCz.[34] Ito and co-workers revealed that the carbazole excimer has continuous energy levels depending on the overlapping of carbazole rings from a study of excimer formation in sterically hindered poly(3,6-di-*tert*-butyl-9-vinylcarbazole).[35,36] Evers and co-workers reported that the partially and fully overlapped excimers are derived independently from *rac*-2,4-bis(*N*-carbazolyl)pentane and *meso*-2,4-bis(*N*-carbazolyl)pentane, which correspond to the syndiotactic and the isotactic dyad in the PVCz chain, respectively.[37] De Schryver studied the formation kinetics of intramolecular excimers in these model compounds by time-resolved fluorescence spectroscopy.[38−40] However, these model compounds do not provide us with a definitive structure of the excimer, because the intramolecular excimers formed need to change their conformation.

Here, we studied the excimer fluorescence of carbazolophanes of which the geometrical alignments of two carbazole moieties are clearly defined: *syn*-[3.3](3,9)carbazolophane has a structure with two carbazole rings fully overlapping each other and *anti*-[3.3](3,9)carbazolophane has a structure with only one benzene ring in a carbazole moiety overlapping with one benzene ring in another carbazole moiety. There have been few studies on carbazole excimers using carbazolophanes,[41−43] although many studies on intramolecular carbazole excimers using carbazole dimeric compounds linked by an alkane chain have been reported. Recently, we reported the synthesis, structure, and fundamental photophysical properties of *syn*- and *anti*-[3.3](3,9)-carbazolophanes.[43] Following the previous study, we investigated the electronic properties of two overlapping carbazole moieties in the excited state by spectroscopic measurements.

2. Experimental Part

Materials. *N*-Ethylcarbazole (EtCz) was synthesized by *N*-alkylation of carbazole and was purified by silica gel column chromatography and recrystallization. 1,3-Bis(*N*-carbazolyl)-propane (DCzPr) was prepared from 1,3-dibromopropane and sodium carbazole and purified by recrystallization from a mixture of dichloromethane and hexane. 1,3-Bis(3-methyl-*N*-carbazolyl)propane (DMeCzPr)[44] was prepared from 1,3-bis-(3-bromomethyl-*N*-carbazolyl)propane[43] and purified by recrystallization from ethanol. We synthesized *syn*- and *anti*-[3.3](3,9)carbazolophanes by intramolecular cyclization of 1,3-bis(3-bromomethyl-*N*-carbazolyl)propane with NH_2CN. Details of the synthesis have been described elsewhere.[43] Solvents used here were 2-methyltetrahydrofuran (MTHF; Nacalai Tesque), cyclohexane (CH; Nacalai Tesque, spectroscopic grade), tetrahydrofuran (THF; Nacalai Tesque, spectroscopic grade), and acetonitrile (MeCN; Nacalai Tesque, spectroscopic grade). Before use, MTHF was dried with solid KOH, passed through freshly activated alumina, and then distilled from CaH_2 with 2,6-di-*tert*-butyl-*p*-cresol. Other solvents were used without further purification. Chemical structures of the carbazole compounds used in this study are shown in Figure 1. Two carbazole moieties in *syn*- and *anti*-[3.3](3,9)carbazolophanes are fully and partially overlapped, respectively. The former is abbreviated as [3.3]Cz-FO and the latter as [3.3]Cz-PO.

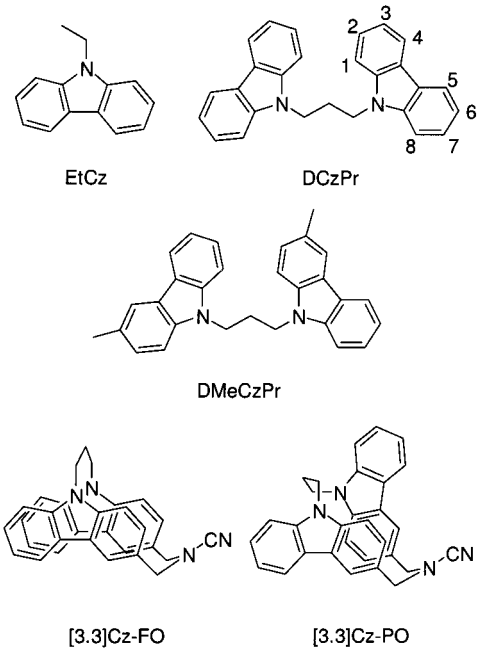

Figure 1. Chemical structures of *N*-ethylcarbazole (EtCz), 1,3-bis(*N*-carbazolyl)propane (DCzPr), 1,3-bis(3-methyl-*N*-carbazolyl)propane (DMeCzPr), *syn*-[3.3](3,9)carbazolophane ([3.3]Cz-FO), and *anti*-[3.3](3,9)carbazolophane ([3.3]Cz-PO).

^{1}H NMR Measurements. ^{1}H NMR spectra were recorded on a Bruker DPX-400 spectrometer with an operating frequency of 400.133 MHz, a spectral width of 8223.68 Hz, and an acquisition time of 1.992 34 s at a temperature of 300.0 K in $CDCl_3$ solvent with tetramethylsilane (TMS) as an internal standard.

Absorption and Fluorescence Measurements. Steady-state absorption and emission spectra were measured at room temperature in a 1-cm quartz cell with a spectrophotometer (Hitachi, U-3500) and a fluorescence spectrophotometer (Hitachi, F-4500), respectively. Samples in the MTHF solvent were degassed by the freeze−pump−thaw method. Samples in other solvents were degassed by Ar bubbling for 30 min. The concentration of carbazole compounds was on the order of 10^{-5} mol/L.

Fluorescence Decay Measurements. Fluorescence decay was measured by the time-correlated single-photon-counting method. A mode-locked Ti:sapphire laser (Spectra-Physics, Tsunami 3950) that was pumped by an Ar^+ laser (Spectra-Physics, BeamLok 2060) provided picosecond pulses (885 nm) at a repetition rate of 82 MHz. The output from the Ti:sapphire oscillator laser was pulse-selected to reduce the repetition rate to 4 MHz and frequency-doubled by a frequency doubler/pulse selection unit (Spectra-Physics, model 3980) and then frequency-tripled (Spectra-Physics, GWU). The generated third-harmonic pulses (295 nm) were used as an excitation light source. The fluorescence emission was collected at 90°, passed through a monochromator (Ritsu, MC-10N) with a cut filter (UV-34) for the excitation light, and detected by a photomultiplier tube (PMT; Hamamatsu Photonics, R3234). The PMT signal was sent to a constant fraction discriminator (ORTEC, model 583) and served as the start pulse for a time-to-amplitude converter (TAC; ORTEC, model 457). The residual SHG pulse was sent into a photodiode (Antel Optronics, AR-32) to provide the stop

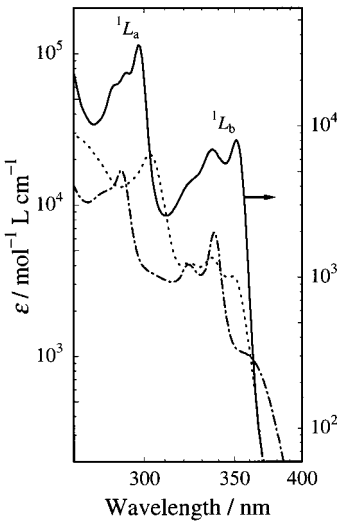

Figure 2. Absorption spectra of DMeCzPr (solid line, right ordinate), [3.3]Cz-PO (dotted line), and [3.3]Cz-FO (dashed−dotted line) in a THF solution at room temperature.

TABLE 1: ^{1}H NMR Chemical Shifts of Aromatic Protons of EtCz, DCzPr, [3.3]Cz-PO, and [3.3]Cz-FO Measured in a $CDCl_3$ Solution at Room Temperature

	H1	H2	H3	H4	H5	H6	H7	H8
EtCz	7.40	7.46	7.22	8.10	8.10	7.22	7.46	7.40
DCzPr	7.19	7.39	7.22	8.10	8.10	7.22	7.39	7.19
[3.3]Cz-PO	5.44	6.41		7.81	8.15	7.33	7.53	7.56
[3.3]Cz-FO	6.98	7.16		7.37	7.47	6.75	6.94	6.98

pulse for the TAC converter through a 100-MHz discriminator (ORTEC, model 436). The TAC signal was transferred to a multichannel analyzer (Norland, IT-5300). The total instrument response function has a fwhm of ca. 750 ps at the excitation wavelength. The decay data were fitted with sums of a function that were convoluted with the instrument response function by the nonlinear least-squares method.

3. Results and Discussion

Molecular Structures in Solutions. ^{1}H NMR spectra were measured for EtCz, DCzPr, [3.3]Cz-PO, and [3.3]Cz-FO in $CDCl_3$ at room temperature to investigate the structures of the carbazolophanes in solution. ^{1}H NMR chemical shifts of aromatic protons of carbazole compounds are summarized in Table 1. The chemical shifts of all aromatic protons in [3.3]-Cz-FO were shifted upfield compared with those of the reference DCzPr. This shows that the two carbazole moieties in [3.3]Cz-FO fully overlap with each other: *syn*-conformation. On the other hand, the chemical shifts of H1 and H2 of the two carbazole moieties in [3.3]Cz-PO were markedly shifted upfield, that of H4 was moderately shifted upfield, and those of other aromatic protons were rather shifted downfield compared with those of DCzPr. These chemical shifts clearly show that the two carbazole rings in [3.3]Cz-PO partially overlap: *anti*-conformation. These assignments were completely in agreement with the X-ray analysis reported elsewhere.[43] Therefore, these results indicate that [3.3]Cz-PO and [3.3]Cz-FO do not flip their carbazole rings and that the anti and syn conformations remain rigid even in solution.

Absorption Spectra. Figure 2 shows the absorption spectra of DMeCzPr, [3.3]Cz-FO, and [3.3]Cz-PO in a THF solution at room temperature. The absorption bands of DMeCzPr at 297 and 351 nm were assigned to the $^1L_a \leftarrow {}^1A$ and $^1L_b \leftarrow {}^1A$ transitions, respectively.[45,46] Absorption spectra of DMeCzPr

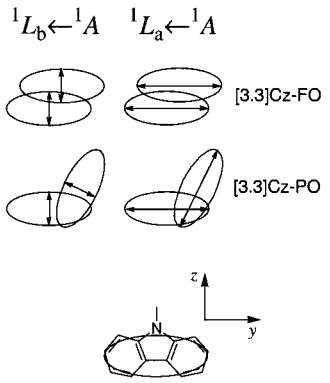

Figure 3. Alignments of transition dipole moments in [3.3]Cz-PO and [3.3]Cz-FO. The ellipsoid corresponds to a carbazole moiety as shown in the bottom figure with the direction coordinate axes for a carbazole moiety. The $^1L_a \leftarrow {}^1A$ transition moments of a carbazole moiety are polarized along the long molecular axis *y*. The $^1L_b \leftarrow {}^1A$ transition moment is polarized along the short molecular axis *z*.

were similar to that of EtCz except for a red-shift of absorption bands owing to substitution of the 3-methyl group. Therefore, there is no electronic interaction between two carbazole moieties in DMeCzPr. However, each absorption band of [3.3]Cz-FO and [3.3]Cz-PO showed broadening and a shift. These findings indicate that the two carbazole moieties electronically interact with each other in the ground state.

The broadening and peak shift observed in [3.3]Cz-FO and [3.3]Cz-PO can be explained by Kasha's exciton coupling theory.[47] First, our attention is focused on [3.3]Cz-FO. As shown in Figure 2, absorption bands corresponding to $^1L_a \leftarrow {}^1A$ and $^1L_b \leftarrow {}^1A$ transitions were all blue-shifted compared with those of DMeCzPr. The $^1L_a \leftarrow {}^1A$ transition moments of a carbazole moiety are known to be polarized along the long molecular axis *y*. The $^1L_b \leftarrow {}^1A$ transition moment is polarized along the short molecular axis *z*.[46] Figure 3 shows that both the short (^1L_b) and long (^1L_a) transition dipoles of a carbazole moiety in [3.3]-Cz-FO are parallel to those of the other carbazole moiety. The interaction of parallel out-of-phase transition dipoles leads to an energy level lower than that of the isolated molecules, while the interaction of parallel in-phase transition dipoles leads to a higher energy level. Transition from the ground state to the lower exciton state (out-of-phase) is forbidden, while transition from the ground state to the higher exciton state (in-phase) is allowed. Therefore, these parallel transition dipoles cause blue-shifted absorption bands. A weak absorption tail observed at wavelengths longer than 350 nm is ascribed to the forbidden transition.

Next, our attention is focused on [3.3]Cz-PO. Figure 2 shows that the absorption band corresponding to the $^1L_a \leftarrow {}^1A$ transition was red-shifted compared with those of DMeCzPr and the absorption intensity of the $^1L_b \leftarrow {}^1A$ transition was weaker than those of DMeCzPr. Figure 3 shows that the angle between long (^1L_a) transition dipoles for [3.3]Cz-PO is more than 90°; this is similar to in-line alignments. On the other hand, the angle between short (^1L_b) transition dipoles is less than 90°; this is similar to parallel alignments. In-line transition dipoles cause red-shifted absorption bands contrary to parallel transition dipoles. Intermediate alignments lead to band-splitting: both transitions to a state of out-of-phase and to a state of in-phase are partially allowed. Qualitatively, it can be safely said that quasi-parallel alignments lead to a blue-shifted band with a weak red-shifted band while quasi-in-line alignments lead to a red-shifted band with a weak blue-shifted band. Therefore, the red-shifted band of the $^1L_a \leftarrow {}^1A$ transition is due to the quasi-in-

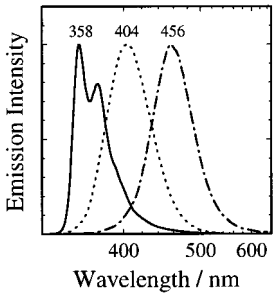

Figure 4. Fluorescence spectra of DMeCzPr (solid line), [3.3]Cz-PO (dotted line), and [3.3]Cz-FO (dashed−dotted line) in a THF solution at room temperature. Emission intensity was normalized.

TABLE 2: Peak Wavelength, λ_{max}, and Peak Shift, $\Delta\tilde{\nu}$, of Excimer Fluorescence from DCzPr, DMeCzPr, [3.3]Cz-PO, and [3.3]Cz-FO Measured in a THF Solution at Room Temperature

	DCzPr	DMeCzPr	[3.3]Cz-PO	[3.3]Cz-FO
λ_{max} (nm)	430[a]	430	404	456
$\Delta\tilde{\nu}$ (cm^{-1})	5400[a]	4677[b]	3108[b]	6003[b]

[a] Taken from refs 31 and 33. [b] Peak shift, $\Delta\tilde{\nu}$, was calculated from a subtraction of $\tilde{\nu}_e$ (peak wavenumber of excimer emission) from $\tilde{\nu}_0$ (peak wavenumber of the (0,0) band of DMeCzPr fluorescence).

line alignments of long (^1L_a) transition dipoles of a carbazole moiety, and the decrease in absorption intensity of the $^1L_b \leftarrow {}^1A$ transition is ascribed to the weak blue-shifted bands, which is partially forbidden. Absorption bands of carbazolophanes well reflect their characteristic structures.

Fluorescence Spectra. Figure 4 shows fluorescence spectra of DMeCzPr, [3.3]Cz-PO, and [3.3]Cz-FO in a MTHF solution at room temperature. The fluorescence spectrum of DMeCzPr (solid line) was clearly ascribed to the carbazole (Cz) monomer emission, which had vibrational bands at 358 and 375 nm. On the other hand, the fluorescence spectra of both [3.3]Cz-PO (dotted line) and [3.3]Cz-FO (dashed−dotted line) showed a red-shifted broad emission band without a vibrational structure. The peak shift from the (0,0) band of the monomer fluorescence of DMeCzPr corresponded to 3108 cm^{-1} in energy for [3.3]-Cz-PO and 6003 cm^{-1} for [3.3]Cz-FO (Table 2). The large peak shift is characteristic of most aromatic excimers, which corresponds to about 6000 cm^{-1} in energy for a large number of aromatic compounds.[4] These broad emissions were also observed even in a MTHF rigid matrix at 77 K where translational diffusion is negligible. Excitation spectra of [3.3]Cz-PO and [3.3]Cz-FO were the same as the absorption spectra. Therefore, these findings indicate that the broad structureless emission of the carbazolophanes is not due to any impurities but is due to intramolecular excimer fluorescence.

The large Stokes shift observed shows that the electronic state in the ground state is quite different from that in the emission state. The carbazolophanes are so rigid that large structural change is highly restricted, but a slight change in their structures causes large energetic stabilization in the excited state leading to excimer formation. The difference between the absorption and emission spectra indicates that the medium coupling between two Cz moieties in the ground state changes to strong coupling in the excited state leading to excimer formation.

The fluorescence spectrum of DMeCzPr in Figure 4 seems to be only monomer fluorescence. However, the oxygen-quenching experiment revealed the fluorescence of both monomer and excimer in the spectrum. The solid line and broken line in Figure 5 show the fluorescence spectra of DMeCzPr after and before Ar bubbling, respectively. The difference in emission

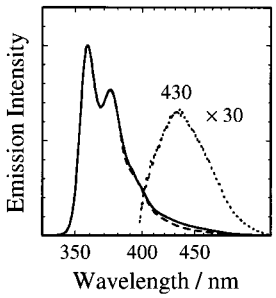

Figure 5. Fluorescence spectra of DMeCzPr in a THF solution at room temperature: after Ar bubbling (solid line); before Ar bubbling (broken line); the subtracted spectrum (dotted line).

intensity was observed around 430 nm: the intensity after Ar bubbling was slightly larger than that before Ar bubbling. The subtracted spectrum (dotted line) of the latter from the former clearly showed an excimer emission band at 430 nm. This peak wavelength was the same as that of DCzPr.[31,32]

The peak shift energy, $\Delta\tilde{\nu}$, is summarized in Table 2. The shift energy of DMeCzPr being smaller than that of DCzPr reflects that steric hindrance of the 3-methyl group leads to the decrease in the stabilization energy in the excited state. The largest energy shift of [3.3]Cz-FO indicates that the shorter distance owing to short [3.3](3,9)linkage results in a larger stabilization energy in the excited state and in a larger repulsion energy in the ground state. This large energy shift of 6003 cm^{-1} indicates that [3.3]Cz-FO in the excited state is stabilized by the charge resonance interaction as well as the molecular exciton interaction. The difference of peak shift between [3.3]Cz-PO and [3.3]Cz-FO indicates that the stabilization energy in the excited states or repulsion energy in the ground state or both of [3.3]Cz-FO are larger than those of [3.3]Cz-PO because two carbazole moieties in [3.3]Cz-FO are fully overlapped while two carbazole moieties in [3.3]Cz-PO are partially overlapped.

Solvent Polarity Effects on Excimer Fluorescence. The carbazolophanes in the excited singlet states are examined in terms of solvent polarity. Excimer fluorescence is insensitive to solvent polarity compared with exciplex emission because the excimer consists of the same molecules in contrast to the exciplex. The solvent polarity dependence of the wavenumber maximum of excimer emissions is well-described by the Lippert−Mataga[48−51] equation (eq 1),

$$\tilde{\nu}_e = \text{const} - \frac{1}{4\pi\epsilon_0}\frac{2}{hc\rho^3}\mu_e^2\left(\frac{\epsilon-1}{2\epsilon+1} - \frac{1}{2}\frac{n^2-1}{2n^2+1}\right)$$
$$= \text{const} - \frac{1}{4\pi\epsilon_0}\frac{2}{hc\rho^3}\mu_e^2 f(\epsilon,n) \quad (1)$$

where $\tilde{\nu}_e$ is the maximum wavenumber of emission, ϵ_0 is the vacuum permittivity, h is the Planck constant, c is the velocity of the light, ρ is the spherical radius of the solute, μ_e is the dipole moment of the solute in the excited state, ϵ is the dielectric constant of the solvent, and n is the refractive index of the solvent.

Figure 6 shows the Lippert−Mataga plots of excimer emissions for [3.3]Cz-PO and [3.3]Cz-FO in several solvents. The maximum wavenumber of excimer emission from the carbazolophanes was insensitive to solvent polarity; the excimer emission of [3.3]Cz-PO was unchanged for all solvents, and that of [3.3]Cz-FO slightly depended on solvent polarity. Thus, the carbazolophanes in the excited states are not as polar as the exciplex or CT complex. The dipole moments of the carbazolophanes in the excited states were estimated to be ~0 D for

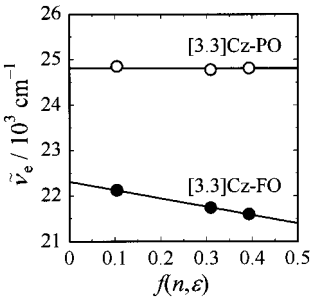

Figure 6. Lippert−Mataga plots of excimer emissions for [3.3]Cz-PO (open circles) and [3.3]Cz-FO (closed circles) in cyclohexane, THF, and acetonitrile at room temperature. Solid lines are fitted to the data by the least-squares method using eq 1.

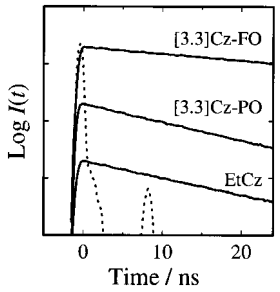

Figure 7. Fluorescence decay curves of EtCz, [3.3]Cz-PO, and [3.3]-Cz-FO in a MTHF solution at room temperature. Excitation wavelength was 295 nm for all samples. Monitor wavelengths were 350 nm for EtCz, 405 nm for [3.3]Cz-PO, and 455 nm for [3.3]Cz-FO. The intensity is shifted lower for [3.3]Cz-PO and EtCz. The dotted line shows an excitation laser pulse.

[3.3]Cz-PO and 4.8 D for [3.3]Cz-FO using eq 1, if the spherical radius, ρ, is assumed to be 5 Å. The difference between the dipole moments in the excited states probably results from the geometrical alignment of their two carbazole moieties: the parallel alignment of [3.3]Cz-FO leads to dipole moment larger than that of the oblique alignment of [3.3]Cz-PO. It is difficult to discuss the absolute value of the dipole moments depending on the spherical radius, ρ, but it can be safely said that the dipole moment of [3.3]Cz-PO in the excited state is negligible within experimental error. This small dipole moment may suggest that mixing of the charge resonance state with the exciton states leads to charge delocalization among the two carbazole rings resulting in a decrease in dipole moment.

Fluorescence Decay Measurements. To examine the excimer state of the carbazolophanes, we measured the fluorescence decay of EtCz, [3.3]Cz-PO, and [3.3]Cz-FO in a MTHF solution. As shown in Figure 7, the fluorescence rise was not observed for any sample within the instrument response function (ca. 750 ps). The same results were obtained even in a MTHF rigid matrix at 77 K. These findings show that excimer formation in carbazolophanes completes within 750 ps after laser excitation and needs only slight structural change. The transition rate from the locally excited state to the excimer state was estimated to be more than 10^9 s^{-1}. The fluorescence decays were fitted to the following equation consisting of two exponential terms by the nonlinear least-squares method:

$$I(t) = G_1 \exp(-t/\tau_1) + G_2 \exp(-t/\tau_2) \qquad (2)$$

The fitting parameters are summarized in Table 3. Although the short lifetime in Table 3 may be ascribed to fast monomer decay due to excimer formation, the fraction is too small to discuss the origin quantitatively. Here, therefore, we focus on long-lifetime components. The radiative rates, k_f, in Table 3

TABLE 3: Fitting Parameters for Fluorescence Decay, Fluorescence Quantum Yield, Radiative Rate, and Nonradiative Rate of EtCz, [3.3]Cz-PO, and [3.3]Cz-FO in a MTHF Solution at Room Temperature

	τ_1 (ns)	τ_2 (ns)	G_1	G_2	χ^2	Φ_f[a]	k_f[c] (s^{-1})	k_n[d] (s^{-1})
EtCz	14.4		1.09		1.27	0.43[b]	3.0×10^7	4.0×10^7
[3.3]Cz-PO	13.7	3.3	1.02	0.04	1.46	0.047	3.4×10^6	6.9×10^7
[3.3]Cz-FO	37.5	2.6	0.99	0.04	1.53	0.027	7.2×10^5	2.6×10^7

[a] The fluorescence quantum yields were determined by comparison with that of EtCz the quantum yield of which is reported to be 0.441 in CH_2Cl_2.[54] [b] Corrected by the refractive index of MTHF. [c] $k_f = \Phi_f/\tau_1$. [d] $k_n = (1 - \Phi_f)/\tau_1$.

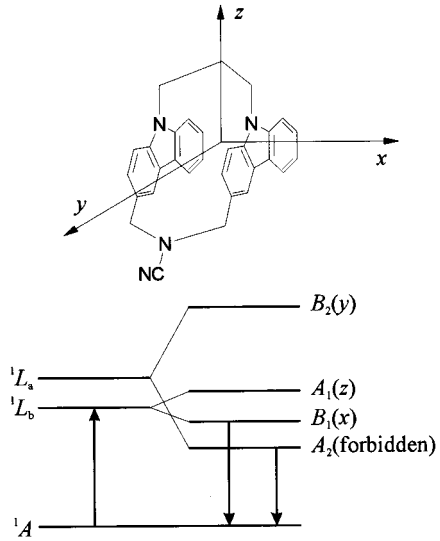

Figure 8. Energy level diagrams of the [3.3]Cz-FO excimer in C_{2v} symmetry.[33] The top figure shows the direction coordinate axes for [3.3]Cz-FO. The left side of the diagram shows energy levels for carbazole monomer: ^{1}A is the ground state and ^1L_a and ^1L_b correspond to the transitions of DMeCzPr. The right side of the diagram shows molecular exciton states derived from the exciton interaction between two carbazole moieties: A_2 and $B_2(y)$ states are derived from ^1L_a states of carbazole monomer, $B_1(x)$ and $A_1(z)$ states are derived from ^1L_b states of carbazole monomer, and x, y, and z in the parentheses show the polarization of the transitions between the corresponding states and the ground state.

are ascribable to those of the intramolecular excimers of [3.3]-Cz-PO and [3.3]Cz-FO because there were no monomer emissions in the steady-state emission spectra of the carbazolophanes and there was no rise in the fluorescence decays. The radiative rates of [3.3]Cz-PO and [3.3]Cz-FO were 3.4×10^6 and 7.2×10^5 s^{-1}, respectively, which were about 1/10 and 1/40 smaller than that of EtCz (3.0×10^7 s^{-1}), while the nonradiative rates, k_n, were on the same order. These slow radiative rates show that excimer emissions of [3.3]Cz-PO and [3.3]Cz-FO are partially forbidden. According to theoretical prediction, the excimer emission of carbazole dimer in C_{2v} symmetry is forbidden. Johnson proposed the energy diagram of a carbazole excimer as shown in Figure 8: the lowest excited state of the carbazole excimer in C_{2v} symmetry is the A_2 state derived from the ^1L_a state of the monomer by molecular exciton interaction, because the exciton interaction between the ^1L_a states is larger than that between the ^1L_b states.[33] The lowest-lying A_2 state of the dimer is not dipole-coupled to the ground state. Therefore, excimer fluorescence of [3.3]Cz-FO in C_{2v} symmetry is ascribed to a transition from the A_2 state to the ground state. The excimer state of [3.3]Cz-FO in C_{2v} symmetry is primarily stabilized by the molecular exciton interaction.[52] On the other hand, the symmetry of [3.3]Cz-PO is lower than that of [3.3]-

Cz-FO. For the dimer configuration of low symmetry, the ^1L_a and ^1L_b molecular exciton states are dipole-coupled to the ground state.[53] Therefore, the excimer fluorescence of [3.3]Cz-PO has a partially dipole-allowed character, resulting in a radiative rate that is faster than that of [3.3]Cz-FO.

4. Conclusion

The photophysical properties of carbazole excimers were investigated using two [3.3](3,9)carbazolophanes ([3.3]Cz-FO and [3.3]Cz-PO). The structures of [3.3]Cz-FO and [3.3]Cz-PO were assigned to fully and partially overlapped conformations, respectively, even in solution, by ^{1}H NMR measurements. Absorption spectra can be explained by Kasha's molecular exciton theory. The solvent polarity effect of the fluorescence spectra revealed that [3.3]Cz-FO in the excited state is slightly polar (4.8 D) while [3.3]Cz-PO in the excited state is nonpolar (∼0 D). The fluorescence decay reflected the difference in symmetry in the excited states between [3.3]Cz-FO and [3.3]-Cz-PO. For [3.3]Cz-FO in C_{2v} symmetry, the large exciton interaction leads to a large red-shifted excimer emission and the symmetry-forbidden transition to the ground state results in a slower radiative rate of the excimer fluorescence. On the other hand, for [3.3]Cz-PO in lower symmetry, the small exciton interaction leads to small red-shifted excimer emission and the partially forbidden transition causes a faster radiative rate of the excimer fluorescence.

Acknowledgment. This work was supported by Grants-in-Aid for Encouragement of Young Scientists (A) (Grant Nos. 10750650 and 12750797) from the Ministry of Education, Science, Sports and Culture of Japan.

References and Notes

(1) Förster, T.; Kasper, K. *Z. Phys. Chem. NF* **1954**, *1*, 275.
(2) Birks, J. B. *Photophysics of Aromatic Molecules*; Wiley-Interscience: London, 1970; Chapter 7.
(3) Klöpffer, W. In *Organic Molecular Photophysics*; Birks, J. B., Ed.; Wiley-Interscience: New York, 1973; Chapter 9.
(4) Birks, J. B.; Lumb, M. D.; Munro, I. H. *Proc. R. Soc. London* **1964**, *A280*, 289.
(5) Azumi, T.; Azumi, H. *Bull. Chem. Soc. Jpn.* **1967**, *40*, 279.
(6) Yanari, S. S.; Bovey, F. A.; Lumry, R. *Nature* **1963**, *200*, 242.
(7) Hirayama, F. *J. Chem. Phys.* **1965**, *42*, 3163.
(8) Vala, M. T.; Haebig, J., Jr.; Rice, S. A. *J. Chem. Phys.* **1965**, *43*, 886.
(9) Nishijima, Y. *J. Polym. Sci., Part C* **1970**, *31*, 353.
(10) Ito, S.; Yamamoto, M.; Nishijima, Y. *Bull. Chem. Soc. Jpn.* **1981**, *54*, 35.
(11) Ito, S.; Yamamoto, M.; Nishijima, Y. *Polym. J.* **1981**, *13*, 791.
(12) Ito, S.; Yamamoto, M.; Nishijima, Y. *Bull. Chem. Soc. Jpn.* **1982**, *55*, 363.
(13) Ito, S.; Yamamoto, M.; Nishijima, Y. *Bull. Chem. Soc. Jpn.* **1984**, *57*, 3295.
(14) Ghiggino, K. P.; Roberts, A. J.; Phillips, D. *Adv. Polym. Sci.* **1981**, *40*, 69.
(15) Semerak, S. N.; Frank, C. W. *Adv. Polym. Sci.* **1984**, *54*, 32.
(16) Cram, D. J.; Cram, J. M. *Acc. Chem. Res.* **1971**, *4*, 204.
(17) Cram, D. J.; Steinberg, H. *J. Am. Chem. Soc.* **1951**, *73*, 5691.
(18) Cram, D. J.; Allinger, N. L.; Steinberg, H. *J. Am. Chem. Soc.* **1954**, *76*, 6132.
(19) Koutecký, J.; Paldus, J. *Collect. Czech. Chem. Commun.* **1962**, *27*, 599.
(20) Vala, M. T.; Hillier, I. H.; Rice, S. A.; Jortner, J. *J. Chem. Phys.* **1966**, *44*, 23.
(21) Hillier, I. H.; Glass, L.; Rice, S. A. *J. Chem. Phys.* **1966**, *45*, 3015.
(22) Longworth, J. L.; Bovey, F. A. *Biopolymers* **1966**, *4*, 1115.
(23) Froines, J. R.; Hagerman, P. J. *Chem. Phys. Lett.* **1969**, *4*, 135.
(24) Yanagidate, M.; Takayama, K.; Takeuchi, M.; Nishimura, J.; Shizuka, H. *J. Phys. Chem.* **1993**, *97*, 8881.
(25) Morita, M.; Kishi, T.; Tanaka, M.; Tanaka, J.; Ferguson, J.; Sakata, Y.; Misumi, S.; Hayashi, T.; Mataga, N. *Bull. Chem. Soc. Jpn.* **1978**, *51*, 3449.
(26) Hayashi, T.; Mataga, N.; Umemoto, T.; Sakata, Y.; Misumi, S. *J. Phys. Chem.* **1977**, *81*, 424.
(27) Nakamura, Y.; Tsuihiji, T.; Mita, T.; Minowa, T.; Tobita, S.; Shizuka, H.; Nishimura, J. *J. Am. Chem. Soc.* **1996**, *118*, 1006.
(28) Nishimura, J.; Nakamura, Y.; Hayashida, Y.; Kudo, T. *Acc. Chem. Res.* **2000**, *33*, 679.
(29) Hoegl, H. *J. Phys. Chem.* **1965**, *69*, 755.
(30) Pearson, J. M.; Stolka, M. *Poly*(*N-vinylcarbazole*); Gordon and Breach: New York, 1981.
(31) Klöpffer, W. *Chem. Phys. Lett.* **1969**, *4*, 193.
(32) Klöpffer, W. *J. Chem. Phys.* **1969**, *50*, 2337.
(33) Johnson, G. E. *J. Chem. Phys.* **1975**, *62*, 4697.
(34) Itaya, A.; Okamoto, K.; Kusabayashi, S. *Bull. Chem. Soc. Jpn.* **1976**, *49*, 2082.
(35) Ito, S.; Takami, K.; Tsujii, Y.; Yamamoto, M. *Makromol. Chem., Rapid Commun.* **1989**, *10*, 79.
(36) Ito, S.; Takami, K.; Tsujii, Y.; Yamamoto, M. *Macromolecules* **1990**, *23*, 2666.
(37) Evers, F.; Kobs, K.; Memming, R.; Terrell, D. R. *J. Am. Chem. Soc.* **1983**, *105*, 5988.
(38) De Schryver, F. C.; Vandendriessche, J.; Toppet, S.; Demeyer, K.; Boens, N. *Macromolecules* **1982**, *15*, 406.
(39) Vandendriessche, J.; Palmans, P.; Toppet, S.; Boens, N.; De Schryver, F. C.; Masuhara, H. *J. Am. Chem. Soc.* **1984**, *106*, 8057.
(40) De Schryver, F. C.; Collart, P.; Vandendriessche, J.; Goedeweeck, R.; Swinnen, A.; Van der Auweraer, M. *Acc. Chem. Res.* **1987**, *20*, 159.
(41) Tani, K.; Tohda, Y.; Hisada, K.; Yamamoto, M. *Chem. Lett.* **1996**, 145.
(42) Nakamura, Y.; Kaneko, M.; Yamanaka, N.; Tani, K.; Nishimura, J. *Tetrahedron Lett.* **1999**, *40*, 4693.
(43) Tani, K.; Tohda, Y.; Takemura, H.; Ohkita, H.; Ito, S.; Yamamoto, M. *Chem. Commun.* **2001**, 1914.
(44) DMeCzPr: colorless powder (from ethanol); mp 160−162 °C.; ^{1}H NMR ($CDCl_3$, 400 MHz, room temperature) δ 2.44 (q, J = 7.3 Hz, 2H, CH_2), 2.53 (s, 6H, CH_3), 4.33 (t, J = 7.3 Hz, 4H, CH_2), 7.09 (d, J = 8.3 Hz, 2H, H1), 7.17−7.23 (m, 6H, ArH), 7.35−7.39 (m, 2H, H7), 7.90 (s, 2H, H4), 8.06 (d, J = 7.6 Hz, 2H, H5).
(45) Platt, J. R. *J. Chem. Phys.* **1949**, *17*, 484.
(46) Johnson, G. E. *J. Phys. Chem.* **1974**, *78*, 1512.
(47) Kasha, M.; Rawls, H. R.; El-Bayoumi, M. A. *Pure Appl. Chem.* **1965**, *11*, 371.
(48) Lippert, V. E. *Z. Naturforsch.* **1955**, *10A*, 541.
(49) Lippert, V. E. *Z. Elektrochem.* **1957**, *61*, 962.
(50) Mataga, N.; Kaifu, Y.; Koizumi, M. *Bull. Chem. Soc. Jpn.* **1955**, *28*, 690.
(51) Mataga, N.; Kaifu, Y.; Koizumi, M. *Bull. Chem. Soc. Jpn.* **1956**, *29*, 465.
(52) The property of the A_2 state in the excimer state does not entirely vanish even if the lowest excitonic state A_2 is mixed by configuration interaction with the charge resonance state. The remaining nature of the A_2 state results in the symmetry-forbidden excimer fluorescence of [3.3]Cz-FO.
(53) McGlynn, S. P.; Armstrong, A. T.; Azumi, T. In *Modern Quantum Chemistry, Part III*; Sinanoğlu, O., Ed.; Academic Press: New York, 1965.
(54) Ohmori, S.; Ito, S.; Yamamoto, M. *Ber. Bunsen-Ges. Phys. Chem.* **1989**, *93*, 815.